



IJRASET

International Journal For Research in
Applied Science and Engineering Technology



INTERNATIONAL JOURNAL FOR RESEARCH

IN APPLIED SCIENCE & ENGINEERING TECHNOLOGY

Volume: 9 Issue: XII Month of publication: December 2021

DOI: <https://doi.org/10.22214/ijraset.2021.39663>

www.ijraset.com

Call:  08813907089

E-mail ID: ijraset@gmail.com

Growth, Structural, Spectral, Thermal, Optical, Second and Third Order Nonlinear Optical Properties of Imidazolium Hydrogen Squarate (IHS) Single Crystal

P. Gayathri¹, J. Jayarubi², K. Kesavan³, P. Prabu⁴

^{1, 2, 3}Department of Physics, Periyar Maniammai Institute of Science and Technology, Thanjavur - 613403, Tamil Nadu, India

⁴No.38, Victoria colony, Medical College Road, Thanjavur - 613403, Tamil Nadu, India

Abstract: Imidazolium hydrogen squarate (IHS) crystal has been grown by slow evaporation solution growth technique at room temperature. The lattice parameters of grown crystal were determined using single crystal X-ray diffraction data and compared with powder XRD. Single crystal XRD shows that the crystal crystallizes in monoclinic system with noncentrosymmetric space group Pc. The crystallinity of the grown crystal was confirmed by X-ray powder diffraction analysis. FT-IR and FT-RAMAN analyses qualitatively confirm the various functional groups present in the grown crystal. The ¹H and ¹³C NMR spectra were recorded to establish the molecular structure. Thermal properties of title crystal were studied by thermogravimetric analysis (TGA) and differential thermal analysis (DTA). The UV-Vis-NIR transmission spectrum was recorded to find the band width of optical transmittance window and the lower cutoff wavelength. The optical band gap value of the material is evaluated to be 5.6 eV. The second harmonic generation efficiency was calculated by the Kurtz and Perry powder method using a Q-switched mode locked Nd: YAG laser emitting 1064 nm laser as source. Finally, Z-scan technique was employed to determine the nonlinear refractive index, nonlinear absorption coefficient and third-order NLO susceptibility to find suitability of the grown crystal in photonics and optoelectronics applications.

Keywords: Single crystal; Powder XRD; thermal analysis; SHG; Z-scan studies

I. INTRODUCTION

The modern crystal growing technique has contributed many good quality nonlinear optical crystals to the telecommunication and other field. The increased demand for frequency conversion crystals in current digital systems like optoelectronics, lasers, data storage systems and optical communications makes researchers to put an effort in identifying crystals that are possessing higher second order nonlinear optical properties [1-3].

The squaric acid crystallize in non-centrosymmetric crystal structure that are expected to possess large second-order susceptibilities [4]. Imidazole has amphoteric property and high polarizability that is expected to contribute more to the optical nonlinearity with other moieties. The optical nonlinearity can be increased[5] by adding the conjugated bonds or substituting donors and acceptors with imidazole, In the case of growth of IHS, the squaric acid protonates the Imidazole molecule. This article reports in detail the growth of IHS crystal and results of various characterizations like FT-IR, FT-Raman, NMR, optical, thermal, second and third order nonlinear optical property.

II. EXPERIMENTAL DETAILS

A. Synthesis and Growth

Single crystal of IHS has been synthesized by slow evaporation solution growth technique from imidazole and squaric acid taken in 1:1 ratio in the deionized water. The saturated solution was stirred for three hours to get homogeneous solution. Then the saturated solution of IHS was filtered into a clean glass beaker and covered by a polythene sheet with few holes on it. The purified solution was kept in an undisturbed environment at room temperature. A transparent single crystal was obtained at the bottom of the beaker after few weeks. The reaction involved in the process may be written as shown in Fig.1. The photograph of as grown single crystal is shown in Fig.2.

B. Characterizations

The grown IHS single crystal was characterized by various characterization techniques. The cell parameters and crystal data of grown crystal were collected using crystal diffractometer equipped with a CCD detector (Bruker Kappa APEX II ULTRA), a rotating anode (Bruker AXS, FR591) with MoK α radiation ($\lambda = 0.71073 \text{ \AA}$). The powder X-ray diffraction analysis on the IHS crystal was carried out in an XPERT-PRO diffractometer with CuK α ($\lambda = 1.5406 \text{ \AA}$) radiation over the range $10 - 80^\circ$. The FT-IR spectrum was recorded in the wavelength region of 400 cm^{-1} and 4000 cm^{-1} by Perkin-Elmer, spectrum one FT-IR spectroscopy by packing samples into KBr pellet.

The Bruker RFS 27 stand alone FT-Raman Spectrometer was used to record FT-Raman spectrum in the range $4000 \text{ cm}^{-1} - 50^{-1}$. The ^1H NMR and ^{13}C NMR spectra of the crystal were recorded by Bruker 300 MHz (Ultrasield)™ instrument using D $_2$ O as solvent. The TG-DTA measurements of the crystal were performed by SDT Q600 V20.9 Build 20 thermal analyzer between 20°C to 800°C in nitrogen atmosphere.

The UV-Vis-NIR optical absorption spectral analysis of LAHS single crystal was carried out between 200 and 1100 nm, using Lambda 25 spectrophotometer. The second harmonic generation efficiency was studied by Kurtz and Perry powder technique using Q switched high energy Nd:YAG Laser with fundamental radiation of 1064 nm as optical source. The third-order nonlinear optical behavior of the crystal was studied by single beam Z-scan method with CW (continuous wave) He-Ne laser beam of wavelength 632.8 nm.

III. RESULTS AND DISCUSSION

A. Single Crystal XRD

The molecular structure of the crystal C $_7$ H $_6$ N $_2$ O $_4$ was refined by the least squares method using anisotropic thermal parameters: R = 3%. The title compound crystallizes with two independent molecules Fig.3. From the single crystal X-ray diffraction measurement, it is found that the IHS crystal belongs to monoclinic system with noncentrosymmetric space group Pc. The unit cell parameters were found to be, $a = 9.3867(7) \text{ \AA}$, $b = 10.9993(9) \text{ \AA}$, $c = 7.5719(6) \text{ \AA}$, $\alpha = \gamma = 90^\circ$ and $\beta = 100.168(3)^\circ$. The volume of unit cell is $769.50(11) \text{ \AA}^3$. For the title compound, data collection was done using the computer program APEX2 [6], cell refinement was done using the computer program APEX2/SAINT [6] and data reduction was done by using SAINT/XPREP [6]. The structure of the title compound was solved by using the computer program SIR92 [7] and refined using SHELXL-97 [8]. The molecular graphics were done using the computer programs ORTEP [9], Mercury [10] and PLATON [11].

B. Powder XRD analysis

The crushed fine powder of IHS crystal was exposed to PXRD analysis. The PXRD pattern of the grown crystal was carried out in the 2θ range from 20° to 80° in Bruker D8 focus X-ray powder diffractometer. The obtained planes were indexed by indx software and shown in Fig.4. The recorded pattern shows the sharp diffraction peaks which provide evidence for good crystalline nature of grown crystal. The lattice parameters were evaluated by the software package of UnitCell. The PXRD confirms that the crystal crystallize in monoclinic system. The lattice parameters are, $a = 9.5382(6) \text{ \AA}$, $b = 10.8999(7) \text{ \AA}$, $c = 7.6012(9) \text{ \AA}$, $\alpha = \gamma = 90^\circ$ and $\beta = 100.153(3)^\circ$. The volume of unit cell is $770.21(8) \text{ \AA}^3$. The lattice parameters identified are consistent with single crystal XRD data.

C. Spectral Analysis

FT-IR and FT-Raman are being effective techniques which qualitatively recognize the existence of certain functional groups in a crystal. The recorded FT-IR and FT-Raman spectra are shown in Fig.5, Fig.6. The region from $3623 \text{ cm}^{-1} - 2700 \text{ cm}^{-1}$ are assigned to OH vibrations of squaric acid and CH vibrations of imidazole. The peak at 3623 cm^{-1} could be assigned to O-H stretching vibration of squaric acid. The peak found at 2424 cm^{-1} is assigned to C-C stretching of squaric acid. The O-H stretching carboxylic group is found at 2216 cm^{-1} . The O-H stretching carboxylic group is found at 2216 cm^{-1} . The O-H stretching carboxylic group is found at 2216 cm^{-1} . The C=O Stretching is observed at 1816 cm^{-1} . The peak at 1646 cm^{-1} is due to C=C stretching of squaric acid. Vibrations of 2N- and 4N-imidazole rings observed at 1578 cm^{-1} . The OH bending of squaric acid and skeleton vibrations of imidazole ring assigned to 1512 . The twisting of NH $_2$ vibration is well recognized due to the peak at 1165 cm^{-1} . The C-N stretching of imidazole is observed at 1050 cm^{-1} . OH out-of-plane deformation of squaric acid shows its characteristics peak at 924 cm^{-1} . Aromatic stretching due to Imidazole is observed at 849 cm^{-1} , 720 cm^{-1} and 631 cm^{-1} .

D. NMR Study

The ^1H NMR and ^{13}C NMR spectra of the crystal were recorded and shown in Fig.7. and Fig.8. respectively. The chemical shifts are represented in δ ppm. The chemical shifts of the crystal assigned and are reported in table.8. The ^1H NMR spectrum shows resonance peak from $\delta = 3.232$ to $\delta = 3.577$ ppm are due to hydrogen attached with OH of squaric acid. The peaks $\delta = 4.854$ ppm and $\delta = 6.386$ ppm corresponds to CH in Imidazol ring. In ^{13}C NMR the peak observed at $\delta = 198.87$ ppm is due to CO in squaric acid. The carbon attached to CH_2 of Imidazole shows its resonance peak at 134.98 ppm, $\delta = 126.99$ ppm, $\delta = 122.21$ ppm. The resonance peak at 42.62 ppm is due to the C=O of squaric acid.

E. Thermal Analysis

Thermogravimetric analysis gives vital information about the thermal stability and different stages of decomposition of the crystal by monitoring the weight change that occurs when the crystal is heated. The recorded TGA and DTA curves of IHS are shown in Fig 9. The initial mass of the crystal subjected to analysis was 4.1620 mg. From the TGA analysis it is clearly seen that the crystal is thermally stable upto 180°C . Hence, the crystal can be used for optical applications below 180°C . The decomposition of the crystal starts at 180°C and nearly completes at 382°C . The final mass left out after the analysis was 0.002679 mg which is 0.06437% of mass of the original sample. The endothermic peak observed near 180°C in DTA curve may correspond to the simultaneous melting and decomposition of the crystal.

F. UV-Vis-NIR Transmittance Spectral Analysis

The optical activeness of the grown crystal was ensured by UV optical absorption spectral analysis that carried out between 200 nm and 1100 nm. The recorded spectrum is shown in Fig.10. The absorption spectrum illustrates that the crystal is transparent in the wavelength range of 300 – 1100 nm. The lower cut-off wavelength of the crystal was found to be 300 nm. This study confirms that the crystal is transparent within a wide range of spectrum from UV to IR region, which enables it to be a potential candidate for optoelectronic applications and the second harmonic generation of the Nd:YAG laser. The spectrum shows an absorption peak at 218nm is due to the $\pi \rightarrow \pi^*$ transition. From the fundamental absorption at 218 nm, the band gap energy of the material is calculated using the formula,

$$E_g = h \frac{C}{\lambda} \times 6.2415 \times 10^{18} \text{eV}$$

where,

h = Planks constant = 6.626×10^{-34} Joules sec

C = Speed of light = 3.0×10^8 meter/sec

λ = Cut off wavelength = 218×10^{-9} meter/sec

The band gap energy of the crystal is found to be 5.6 eV. This indicates that the crystal has dielectric behavior to induce polarization when powerful radiation is incident on the material.

G. SHG Efficiency

The grown crystal was subjected to Kurtz and Perry [12] powder second harmonic generation measurement to ensure the crystal in SHG applications. Nd:YAG laser emitting fundamental radiation of 1064 nm, with a pulse width of 10 ns and repetition rate of 10Hz was allowed to pass through the sample. The grown crystal was powdered with a uniform particle size and packed in a microcapillary tube of uniform diameter and exposed to laser radiation. The second harmonics generated in the crystal was confirmed by the emission of green radiation from the crystal with the intensity of 532 nm wavelength. The second harmonic generation efficiency of KDP was also studied, and it is used as the reference for the present study. The efficiency of second harmonic generation of IHS crystal was found to be 0.56 times that of reference material KDP. The SHG analysis suggests suitability IHS crystal for various optoelectronic applications.

H. Z-scan Study

The third-order nonlinear optical behavior of the crystal was studied by single beam Z-scan method with CW (continuous wave) He-Ne laser beam of wavelength 632.8 nm. The z-scan method is a simple and reliable method to determine the nonlinear optical parameters of a material. It provides valid information to find the suitability of material for a particular experimental setup. The normalized transmittance spectra of open and closed aperture of IHS crystal is shown in Fig.11 and Fig.12 respectively. Nonlinear two-photon absorption coefficient was determined from open aperture measurement and nonlinear refraction was determined from closed aperture measurements.

From these measurements the real and imaginary parts of the third-order nonlinear optical susceptibility can be calculated. In the fig.12 the negative phase shift indicates that the valley trails the peak and it is understood that the crystal exhibits strong self defocusing behaviour and negative sign of nonlinear refractive index. This crystal can be used in protection of optical sensors like night vision devices [13]. The reverse saturable absorption behaviour of the crystal is demonstrated by the formation of valley at the focus ($Z=0$). and hence it can be used in optical pulse shorteners and optical energy limiters. The third-order nonlinear optical parameters of IHS crystal was calculated from Z-scan analysis, nonlinear refractive index (n_2) is $-1.2106 \times 10^{-10} \text{ cm}^2/\text{W}$, nonlinear absorption coefficient (β) is $4.1219 \times 10^{-4} \text{ cm/W}$ and nonlinear optical susceptibility $\chi^{(3)}$ is $1.2952 \times 10^{-7} \text{ esu}$.

IV. CONCLUSION

The title crystal was grown by slow evaporation solution growth technique. It is concluded from XRD and powder XRD that the crystal IHS is belongs to monoclinic crystal system with noncentrosymmetry space group Pc. FT-IR and FT-Raman spectroscopy technique confirmed the characteristics vibrations of various functional groups existing in IHS crystal. The ^{13}C NMR, ^1H NMR discloses the hydrogen and carbon environments of the grown crystal. Thermogravimetric (TG) / Differential scanning calorimetry (DSC) analysis reveals that IHS is melting at 180°C . The second harmonic generation (SHG) efficiency of grown crystal was determined after applying Kurtz and Perry powder test. Finally the Z-scan measurement reveals that the crystal exhibits self defocusing and the reverse saturable absorption behaviour of the crystal.

REFERENCES

- [1] H.Zhang, D.E.Zelmon, G.E.Price, B.K.Teo, Inorg. Chem. 39(2000) 1868-1873.
- [2] G.Boyd, Applications requirement for non linear optical devices and status of organic materials, J.Opt.Soc. Am B Opt Phys 1989: 6(4): 685-92
- [3] D.J.Williams, Organic polymeric and non polymeric materials with large optical non linearities. Angew Chem Int Ed 1984:23(9): 690-704.
- [4] M. Spassova, T. Kolev, I. Kanev, D. Jacquemin, B. Champagne, J. Mol. Struct.(THEOCHEM) 528 (2000) 151-159.
- [5] Raval, Hiral; Parekh, B. B.; Parikh, K. D.; Joshi, M. J. (2019). Growth and Characterizations of Organic NLO Imidazolium L-Tartrate (IMLT) Single Crystal. Advances in Condensed Matter Physics, 2019(), 1-9. doi:10.1155/2019/3853215
- [6] Bruker, SAINT-Plus, XPREP and SADABS, Bruker AXS Inc., Madison, WI, USA,2004.
- [7] M.C. Burla, M. Camalli, B. Carrozzini, G.L. Casciarano, C. Giacovazzo, G. Polidori, R. Spagna, J. Appl. Crystallogr. 36 (2003) 1103.
- [8] G.M. Sheldrick, Acta Crystallogr. A 64 (2008) 112-122.
- [9] L.J. Farrugia, J. Appl. Crystallogr. 45 (2012) 849-854.
- [10] I.J. Bruno, J.C. Cole, P.R. Edgington, M. Kessler, C.F. Macrae, P. McCabe, J. Pearson, R. Taylor, Acta Crystallogr. B 58 (2002) 389-397.
- [11] A.L. Spek, Acta Crystallogr. D 65 (2009) 148-155.
- [12] S.K. Kurtz, T.T. Perry, A powder technique for the evaluation of nonlinear optical materials, J. Appl. Phys. 39 (1968) 3798-3814.
- [13] Yun Shan Zhou, En Bo Wang, Jung Peng, Polyhedron 18, (1999) 1419-1423. [DOI: 10.1016/S0277-5387(98)00448-3.

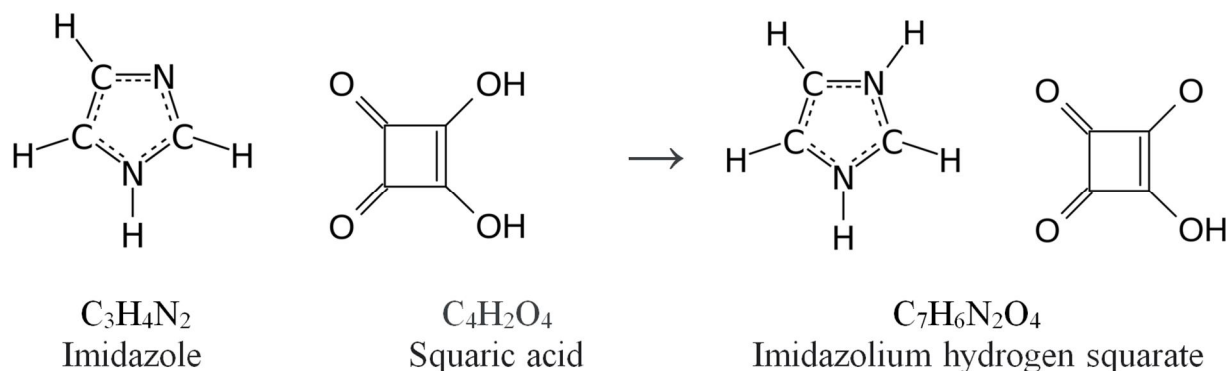


Fig.1 Reaction scheme of IHS single crystal

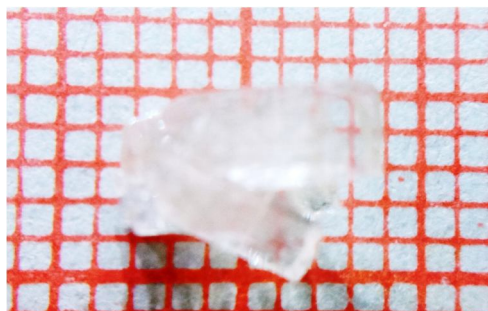


Fig.2 Photo of as grown IHS single crystal

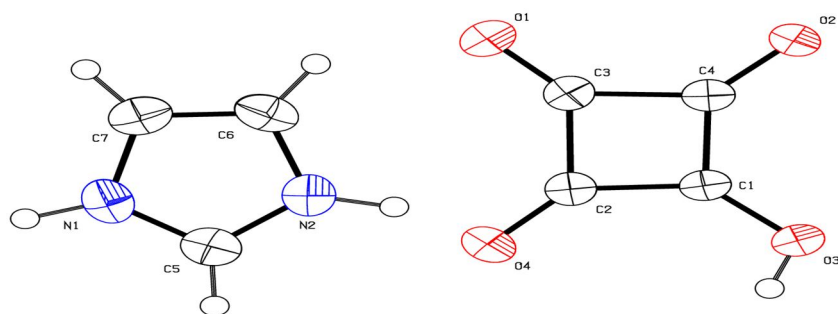


Fig.3 Molecular structure of IHS single crystal

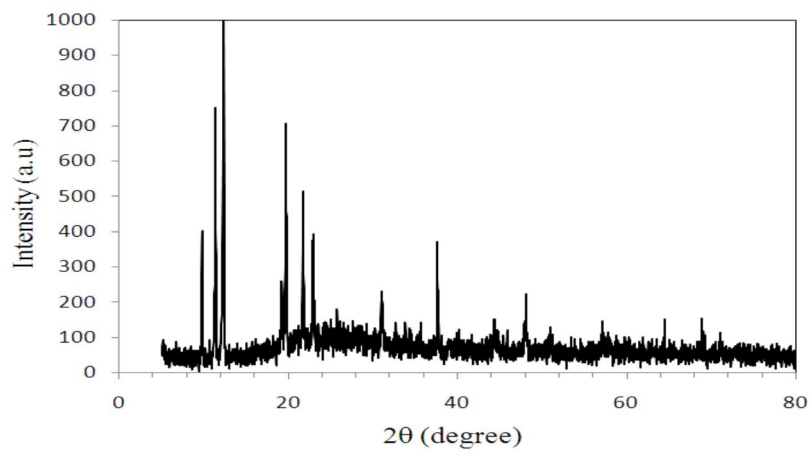


Fig.4 Powder XRD pattern of IHS single crystal

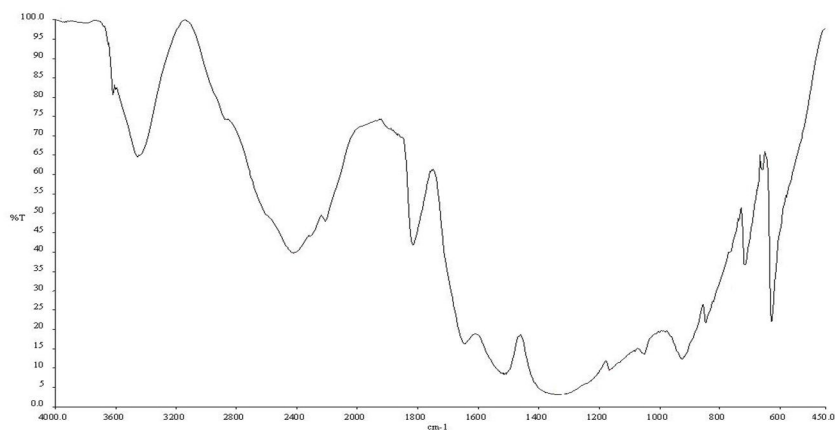


Fig.5 FT-IR spectrum of IHS crystal

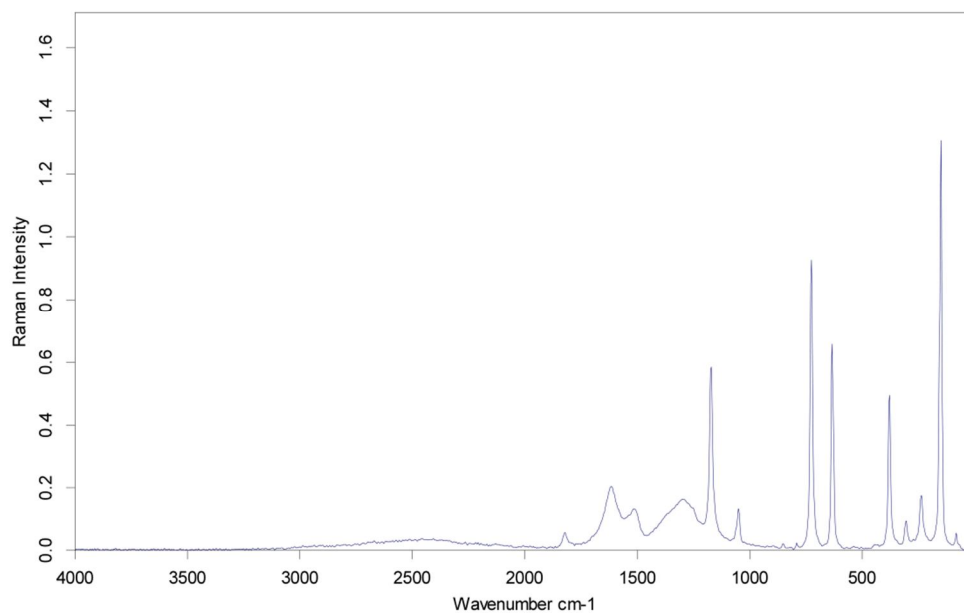


Fig.6 FT-Raman spectrum of IHS crystal

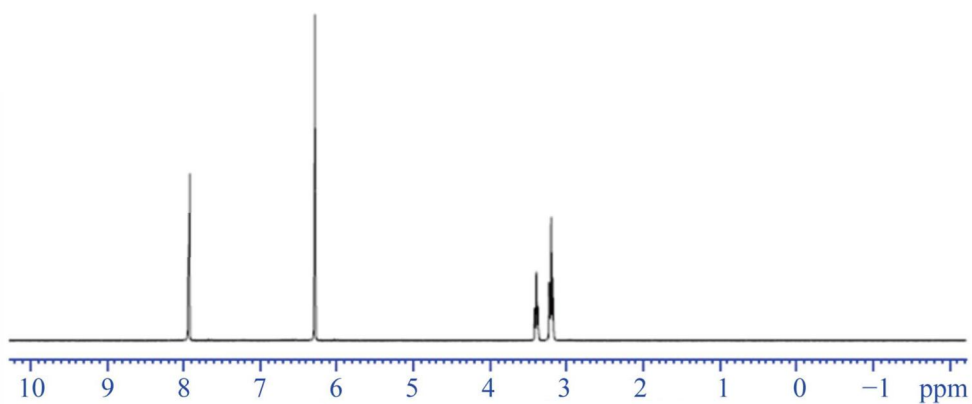


Fig.7 ¹H NMR spectrum of IHS crystal

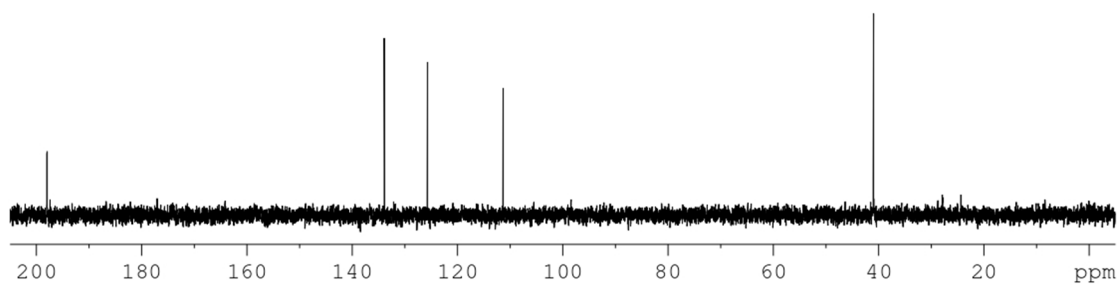


Fig.8 ¹³C NMR spectrum of IHS crystal

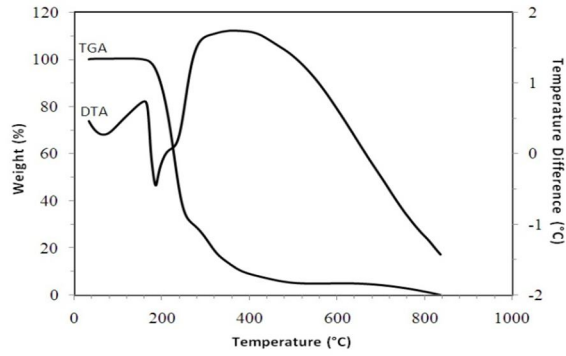


Fig.9 TG/DTA Spectrum of IHS

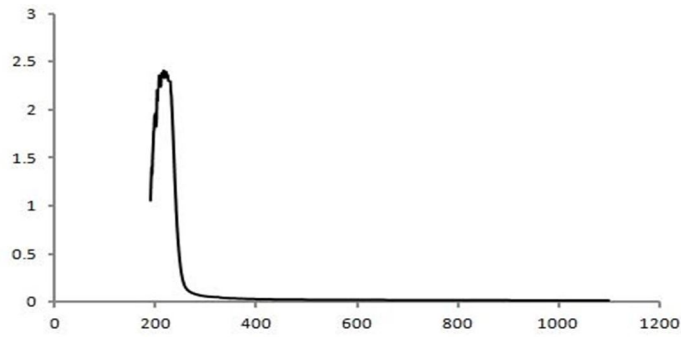


Fig.10 UV-Vis-NIR transmittance spectrum of IHS crystal

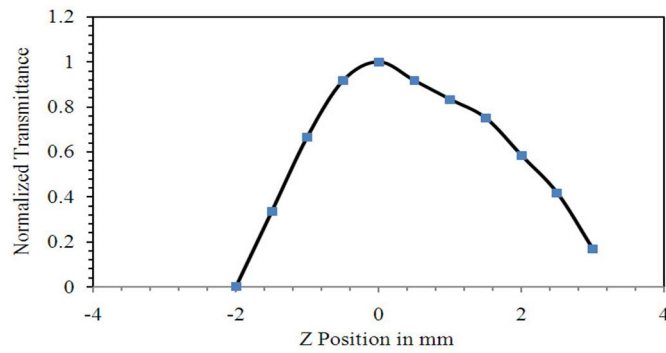


Fig.11 Open aperture curve of IHS crystal

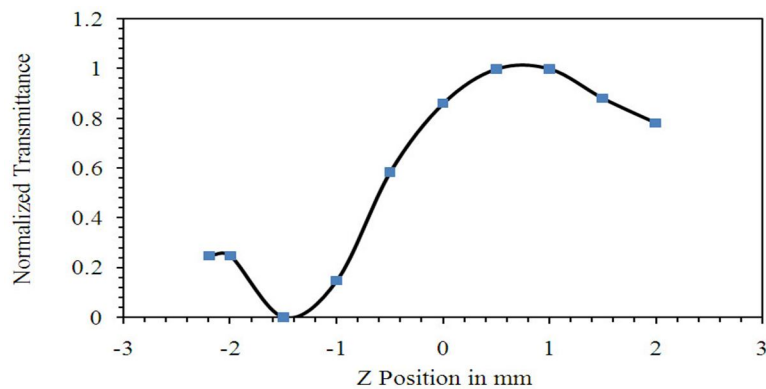


Fig.12 Closed aperture curve of IHS crystal

Table 1 Crystal data and structure refinement for IHS crystal.

Identification code	shelx
Empirical formula	C ₇ H ₆ N ₂ O ₄
Formula weight	182.14
Temperature	296(2) K
Wavelength	0.71073 Å
Crystal system	Monoclinic
Space group	Pc
Unit cell dimensions	a = 9.3867(7) Å
	b = 10.9993(9) Å
	c = 7.5719(6) Å
	α = 90°.
	β = 100.168(3)°.
	γ = 90°.
Volume	769.50(11) Å ³
Z	4
Density (calculated)	1.572 Mg/m ³
Absorption coefficient	0.132 mm ⁻¹
F(000)	376
Crystal size	0.400 x 0.300 x 0.250 mm ³
Theta range for data collection	3.693 to 25.988°.
Index ranges	-11<=h<=11, -13<=k<=13, -9<=l<=9
Reflections collected	12479
Independent reflections	1504 [R(int) = 0.0641]
Completeness to theta = 25.242°	99.40%
Absorption correction	Semi-empirical from equivalents
Max. and min. transmission	0.7454 and 0.6191
Refinement method	Full-matrix least-squares on F ²
Data / restraints / parameters	1504 / 0 / 128
Goodness-of-fit on F ²	1.075
Final R indices [I>2σ(I)]	R1 = 0.0667, wR2 = 0.1735
R indices (all data)	R1 = 0.1015, wR2 = 0.2137
Extinction coefficient	0.065(17)
Largest diff. peak and hole	0.332 and -0.340 e.Å ⁻³

Table 2. Atomic coordinates ($\times 10^4$) and equivalent isotropic displacement parameters ($\text{\AA}^2 \times 10^3$) for IHS. $U(\text{eq})$ is defined as one third of the trace of the orthogonalized U^{ij} tensor.

C(1)	9229(3)	6782(2)	2406(4)	38(1)
C(2)	7829(3)	6821(2)	2915(4)	39(1)
C(3)	7864(3)	8178(2)	2753(4)	41(1)
C(4)	9306(3)	8055(2)	2227(4)	38(1)
C(5)	3513(3)	6430(3)	4897(5)	55(1)
C(6)	4227(3)	8295(3)	4621(5)	53(1)
C(7)	2975(4)	8343(3)	5240(5)	53(1)
N(1)	2547(3)	7151(3)	5400(4)	50(1)
N(2)	4549(3)	7094(3)	4422(4)	49(1)
O(1)	7051(2)	9009(2)	2969(4)	59(1)
O(2)	10231(2)	8780(2)	1802(3)	49(1)
O(3)	10158(2)	5939(2)	2141(4)	54(1)
O(4)	6955(2)	6087(2)	3342(3)	55(1)

Table 3. Bond lengths [\AA] and angles [$^\circ$] for isa.

C(1)-O(3)	1.313(3)
C(1)-C(4)	1.410(4)
C(1)-C(2)	1.434(4)
C(2)-O(4)	1.234(3)
C(2)-C(3)	1.498(4)
C(3)-O(1)	1.220(3)
C(3)-C(4)	1.483(4)
C(4)-O(2)	1.262(3)
C(5)-N(1)	1.311(4)
C(5)-N(2)	1.316(4)
C(5)-H(5)	0.9300
C(6)-C(7)	1.341(5)
C(6)-N(2)	1.370(4)
C(6)-H(6)	0.9300
C(7)-N(1)	1.383(4)
C(7)-H(7)	0.9300
N(1)-H(1)	0.92(4)
N(2)-H(2)	0.92(4)
O(3)-H(3)	0.8200
O(3)-C(1)-C(4)	129.9(2)
O(3)-C(1)-C(2)	136.6(2)
C(4)-C(1)-C(2)	93.5(2)
O(4)-C(2)-C(1)	137.2(3)
O(4)-C(2)-C(3)	134.3(2)
C(1)-C(2)-C(3)	88.5(2)
O(1)-C(3)-C(4)	136.6(3)
O(1)-C(3)-C(2)	135.4(2)

C(4)-C(3)-C(2)	88.0(2)
O(2)-C(4)-C(1)	134.5(2)
O(2)-C(4)-C(3)	135.5(2)
C(1)-C(4)-C(3)	90.0(2)
N(1)-C(5)-N(2)	109.1(3)
N(1)-C(5)-H(5)	125.5
N(2)-C(5)-H(5)	125.5
C(7)-C(6)-N(2)	107.5(3)
C(7)-C(6)-H(6)	126.3
N(2)-C(6)-H(6)	126.3
C(6)-C(7)-N(1)	106.2(3)
C(6)-C(7)-H(7)	126.9
N(1)-C(7)-H(7)	126.9
C(5)-N(1)-C(7)	108.7(3)
C(5)-N(1)-H(1)	130(2)
C(7)-N(1)-H(1)	121(2)
C(5)-N(2)-C(6)	108.5(3)
C(5)-N(2)-H(2)	131(3)
C(6)-N(2)-H(2)	120(3)
C(1)-O(3)-H(3)	109.5

Symmetry transformations used to generate equivalent atoms:

Table 4. Anisotropic displacement parameters ($\text{\AA}^2 \times 10^3$) for IHS. The anisotropic displacement factor exponent takes the form: -
 $2p^2 [h^2 a^* 2U^{11} + \dots + 2 h k a^* b^* U^{12}]$

	U ¹¹	U ²²	U ³³	U ²³	U ¹³	U ¹²
C(1)	37(1)	24(1)	58(2)	0(1)	16(1)	1(1)
C(2)	38(1)	28(1)	56(2)	1(1)	17(1)	1(1)
C(3)	36(1)	30(2)	58(2)	1(1)	16(1)	2(1)
C(4)	39(1)	26(1)	53(2)	0(1)	16(1)	0(1)
C(5)	51(2)	38(2)	81(2)	5(2)	24(2)	-2(1)
C(6)	55(2)	37(2)	71(2)	-2(2)	22(2)	-12(2)
C(7)	55(2)	37(2)	71(2)	-7(2)	20(2)	2(2)
N(1)	39(1)	50(2)	65(2)	-1(1)	20(1)	-6(1)
N(2)	41(1)	44(2)	67(2)	0(1)	21(1)	1(1)
O(1)	53(1)	32(1)	101(2)	0(1)	37(1)	7(1)
O(2)	42(1)	27(1)	83(2)	1(1)	30(1)	-3(1)
O(3)	49(1)	25(1)	98(2)	1(1)	37(1)	4(1)
O(4)	47(1)	34(1)	91(2)	6(1)	33(1)	-5(1)

Table 5. Hydrogen coordinates (x 10⁴) and isotropic displacement parameters ($\text{\AA}^2 \times 10^3$) for IHS.

H(5)	3473	5586	4878	66
H(6)	4776	8957	4371	64

H(7)	2492	9039	5509	64
H(3)	9902	5282	2490	82
H(1)	1720(40)	6960(30)	5850(50)	59(10)
H(2)	5390(40)	6870(40)	4030(50)	78(12)

Table 6. Torsion angles [°] for IHS.

O(3)-C(1)-C(2)-O(4)	1.9(7)
C(4)-C(1)-C(2)-O(4)	-179.1(4)
O(3)-C(1)-C(2)-C(3)	-179.3(4)
C(4)-C(1)-C(2)-C(3)	-0.3(2)
O(4)-C(2)-C(3)-O(1)	-0.8(6)
C(1)-C(2)-C(3)-O(1)	-179.6(4)
O(4)-C(2)-C(3)-C(4)	179.1(4)
C(1)-C(2)-C(3)-C(4)	0.3(2)
O(3)-C(1)-C(4)-O(2)	-0.9(6)
C(2)-C(1)-C(4)-O(2)	-180.0(4)
O(3)-C(1)-C(4)-C(3)	179.4(3)
C(2)-C(1)-C(4)-C(3)	0.3(2)
O(1)-C(3)-C(4)-O(2)	-0.1(7)
C(2)-C(3)-C(4)-O(2)	180.0(4)
O(1)-C(3)-C(4)-C(1)	179.6(4)
C(2)-C(3)-C(4)-C(1)	-0.3(2)
N(2)-C(6)-C(7)-N(1)	-0.4(4)
N(2)-C(5)-N(1)-C(7)	0.2(4)
C(6)-C(7)-N(1)-C(5)	0.1(4)
N(1)-C(5)-N(2)-C(6)	-0.4(4)
C(7)-C(6)-N(2)-C(5)	0.5(4)

Symmetry transformations used to generate equivalent atoms:

Table 7. Hydrogen bonds for isa [Å and °].

D-H...A	d(D-H)	d(H...A)	d(D...A)	<(DHA)
C(5)-H(5)...O(4)#1	0.93	2.36	3.138(4)	141.5
C(6)-H(6)...O(1)	0.93	2.55	3.221(4)	129.6
C(7)-H(7)...O(1)#2	0.93	2.44	3.215(4)	140.8
O(3)-H(3)...O(2)#3	0.82	1.75	2.552(3)	166.6
N(1)-H(1)...O(2)#4	0.92(4)	1.87(4)	2.778(3)	167(3)
N(2)-H(2)...O(4)	0.92(4)	1.86(4)	2.765(3)	167(4)

Symmetry transformations used to generate equivalent atoms:

- #1 -x+1,-y+1,-z+1 #2 -x+1,-y+2,-z+1 #3 -x+2,y-1/2,-z+1/2
- #4 x-1,-y+3/2,z+1/2

Table 8 ^1H NMR and ^{13}C NMR chemical shift assignments of HIS crystal

Spectra	Chemical shift (δ ppm)	Group identification
^1H NMR	3.232 – 3.577	Hydrogen attached with OH of squaric acid
	4.854, 6.386	CH in Imidazol ring
^{13}C NMR	198.87	CO of squaric acid
	134.98, 126.99, 122.21	CH_2 of Imidazole
	42.62	C=O of squaric acid



10.22214/IJRASET



45.98



IMPACT FACTOR:
7.129



IMPACT FACTOR:
7.429



INTERNATIONAL JOURNAL FOR RESEARCH

IN APPLIED SCIENCE & ENGINEERING TECHNOLOGY

Call : 08813907089  (24*7 Support on Whatsapp)